

Multi-decadal trends in the advection and mixing of natural carbon in the Southern Ocean

Nicole S. Lovenduski,¹ Matthew C. Long,² Peter R. Gent,² and Keith Lindsay²

Received 5 November 2012; accepted 29 November 2012; published 2 January 2013.

[1] Multi-decadal trends in the advection, mixing, and air-sea flux of natural carbon dioxide (CO₂) in the Southern Ocean are investigated using output from a hindcast simulation of a non-eddy-resolving ocean model. Particular emphasis is placed on the model's improved eddy-induced advection parameterization. From 1958 to 2007, the model predicts a significant increase in the outgassing of natural CO₂ from the Southern Ocean, congruent with a positive trend in the wind speed over this period. The natural CO₂ flux trend is largely driven by enhanced Eulerian-mean advection and diapycnal mixing of dissolved inorganic carbon (DIC) into the Southern Ocean surface. The natural CO₂ flux trend would be larger, if not for an increase in the eddy-induced advection of DIC out of the Southern Ocean surface, caused by the multi-decadal increase in the model's eddy-induced advection coefficient. **Citation:** Lovenduski, N. S., M. C. Long, P. R. Gent, and K. Lindsay (2013), Multi-decadal trends in the advection and mixing of natural carbon in the Southern Ocean, *Geophys. Res. Lett.*, 40, 139–142, doi:10.1029/2012GL054483.

1. Introduction

[2] It is estimated that the ocean stores about 38,000 Pg of natural dissolved inorganic carbon (DIC), the component of DIC that is in balance with pre-industrial atmospheric carbon dioxide (CO₂) [Denman *et al.*, 2007]. In the Southern Ocean, ventilation along isopycnals connects DIC-rich Circumpolar Deep Water to the surface, permitting natural CO₂ stored in the deep ocean to escape to the atmosphere.

[3] Coarse-resolution ($\Delta x \approx 100$ km) ocean models predict increased outgassing of natural CO₂ from the Southern Ocean in recent decades, due to strengthening westerly winds and enhanced upwelling and equatorward transport of DIC-rich waters [e.g., Le Quéré *et al.*, 2007; Lovenduski *et al.*, 2008]. However, recent literature questions whether coarse-resolution ocean models with parameterized eddies can simulate an appropriate Southern Ocean circulation response to increasing wind intensity [e.g., Böning *et al.*, 2008; Hogg *et al.*, 2008]. The multi-decadal increase in the Eulerian-mean meridional overturning circulation predicted

by eddy-resolving models (associated with upwelling and equatorward transport near the surface) is strongly compensated by a simultaneous increase in the eddy-driven meridional overturning circulation (associated with poleward transport near the surface), such that there is only a small net change in the residual-mean overturning circulation of the Southern Ocean as the wind intensity increases [Marshall and Radko, 2003].

[4] Farneti and Gent [2011] and Gent and Danabasoglu [2011] suggest that the key to obtaining an appropriate Southern Ocean circulation response to stronger winds in a coarse-resolution model is to specify a variable eddy-induced advection coefficient, κ (used in the Gent and McWilliams [1990] parameterization; also known as the thickness diffusivity). Here, we assess the impact of a multi-decadal increase in wind intensity on the advection, mixing, and air-sea exchange of natural carbon in the Southern Ocean using a coarse-resolution ocean model with variable κ . While there is uncertainty over the exact magnitude of the trend in wind, our analysis is aimed at characterizing the mechanisms governing the ocean carbon cycle response to this type of forcing.

2. Methods

[5] We analyze output from a hindcast simulation (1958–2007) (M. C. Long *et al.*, Oceanic carbon uptake and storage in CESM1-BGC, accepted for publication *Journal of Climate*, 2012) of the Community Earth System Model physical ocean component [Danabasoglu *et al.*, 2012] with embedded biogeochemistry and ecology [Moore *et al.*, 2004; Doney *et al.*, 2009]. The model uses 1° horizontal resolution and 10 m vertical resolution in the upper 160 m with 60 total vertical levels. Physical transport terms are partitioned into resolved and unresolved components. Mesoscale eddy transport (isopycnal mixing) is parameterized with an updated version of Gent and McWilliams [1990], where the coefficient κ is diagnosed as function of space and time, rather than prescribed as a constant value [Danabasoglu *et al.*, 2012]. κ is large in the upper mixed layer and then reduces in depth as the square of the buoyancy frequency. Stronger (weaker) surface winds cause a deeper (shallower) mixed layer, which results in a larger (smaller) vertically averaged κ . We perform statistical analysis on model output to determine temporal trends and to quantify the relationship between trends in different variables. Further details on the model configuration and analysis techniques are in the auxiliary material.

3. Results

[6] The ocean model wind stress forcing is based on atmospheric reanalyses, which show an increase in surface wind speed over the Southern Ocean between 1958 and 2007 (Figure 1a). As a result, the model sea-air CO₂ flux exhibits

¹Department of Atmospheric and Oceanic Sciences and Institute of Arctic and Alpine Research, University of Colorado, Boulder, Colorado, USA.

²Climate and Global Dynamics Division, National Center for Atmospheric Research, Boulder, Colorado, USA.

Corresponding author: N. S. Lovenduski, Department of Atmospheric and Oceanic Sciences and Institute of Arctic and Alpine Research, University of Colorado, Campus Box 450, Boulder, CO 80309, USA. (nicole.lovenduski@colorado.edu)

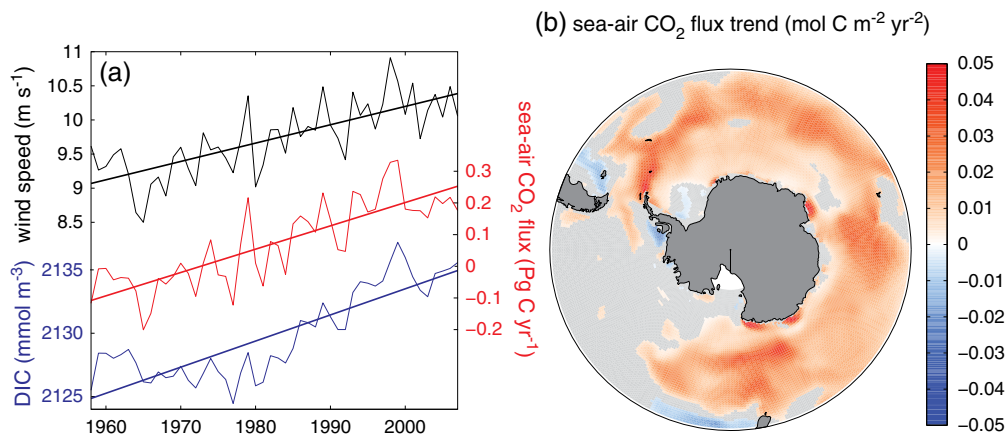


Figure 1. (a) Temporal evolution of annually averaged wind speed, integrated sea-air CO_2 flux, and average surface DIC concentration in the Southern Ocean. (b) Statistically significant linear trends in the flux of CO_2 out of the Southern Ocean surface from 1958 to 2007.

a significant positive trend of $0.007 \pm 0.002 \text{ Pg C yr}^{-2}$, equivalent to a $0.368 \text{ Pg C yr}^{-1}$ increase in the flux over the 50 year simulation (Figure 1a). A spatial map of the CO_2 flux trend (Figure 1b) indicates that it is positive over a large fraction of the Southern Ocean, with the exception of the Eastern Pacific sector, where there are no statistically significant trends. Nearly 60% of the spatially integrated CO_2 flux trend is linearly congruent with the trend in mean surface wind speed over the Southern Ocean during this period, suggesting that the CO_2 flux trend is related to the increase in wind speed.

[7] To ascertain the mechanisms responsible for the trend in the sea-air flux of natural CO_2 , the contributions to the flux trend are estimated using a linear Taylor expansion (see auxiliary material). Increasing surface DIC is the dominant driver of the Southern Ocean CO_2 flux trend (Figure 1a and Table S1). This is countered to a large degree by the trend toward increasing alkalinity, while the impacts of trends in pressure, temperature, salinity, and neglected higher-order terms on the CO_2 flux trend are quite small, but non-negligible. These results are consistent with the findings of Lovenduski *et al.* [2008].

[8] The mechanisms driving changes in surface DIC are investigated by considering the volume-integrated inventory of DIC in the top 100 m of the Southern Ocean, $\text{DIC}_{100\text{m}}$, and its sources and sinks,

$$\frac{\partial \text{DIC}_{100\text{m}}}{\partial t} = J_{\text{adv}} + J_{\text{iso}} + J_{\text{dia}} + J_{\text{gas}} + J_{\text{bio}}, \quad (1)$$

Table 1. Linear Trends in the Southern Ocean-Integrated Sources and Sinks of $\text{DIC}_{100\text{m}}$ as in (1)^a

Term in (1)	Linear Trend	Congruent with Wind
J_{adv}	1.01 ± 0.24	0.75 ± 0.20
J_{iso}	-0.09 ± 0.01	-0.01 ± 0.08
J_{dia}	0.12 ± 0.11	0.09 ± 0.12
J_{gas}	-0.74 ± 0.16	-0.41 ± 0.13
J_{bio}	-0.12 ± 0.08	-0.06 ± 0.09

^aAlso shown is the DIC flux trend that is linearly congruent with the trend in wind speed. Units are $10^{-2} \text{ Pg C yr}^{-2}$, and uncertainty is reported as 95% confidence intervals.

where J_{adv} , J_{iso} , J_{dia} , J_{gas} , and J_{bio} represent the fluxes of DIC from Eulerian advection, isopycnal mixing (i.e., parameterized mesoscale eddy effects), diapycnal mixing, air-sea exchange, and net community production, respectively. The multi-decadal increase in $\text{DIC}_{100\text{m}}$ is caused by positive trends in the advection and diapycnal mixing of DIC (Table 1) over most of the Southern Ocean (Figures 2 and S2). A large fraction of the trends in J_{adv} and J_{dia} , 74% and 75%, respectively, are linearly congruent with wind speed, indicating that the trend in wind plays an important role in the increased advection and diapycnal mixing of Southern Ocean DIC. Trends in the isopycnal mixing, gas exchange, and biological DIC terms are mostly negative throughout the Southern Ocean (Table 1 and Figure S2), countering the effect of advection and diapycnal mixing—both locally and aggregated to the basin scale (Figure 2). Over the course of the simulation, the DIC inventory in the surface ocean increases by 0.6 Pg C , due to enhanced vertical advection that is not entirely compensated for by lateral advection and increases in isopycnal mixing (Figure 2).

[9] The parameterized eddy isopycnal mixing includes two components. The first is the “Redi” term, which mixes

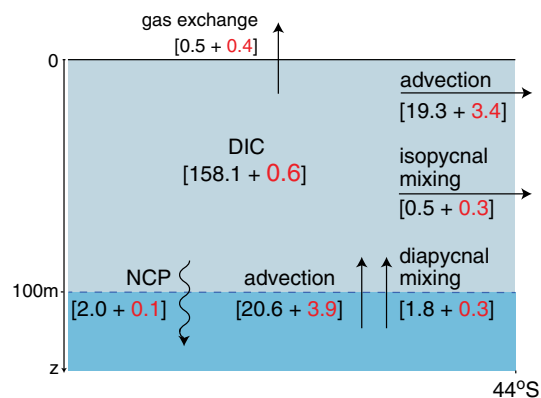


Figure 2. Schematic illustration of the Southern Ocean surface DIC inventory, $\text{DIC}_{100\text{m}}$ (Pg C), and its sources and sinks (Pg C yr^{-1}). Black numbers represent mean values during the first 10 years of the simulation; red numbers represent the total change during the 50 year simulation. Isopycnal mixing is the sum of its horizontal and vertical components.

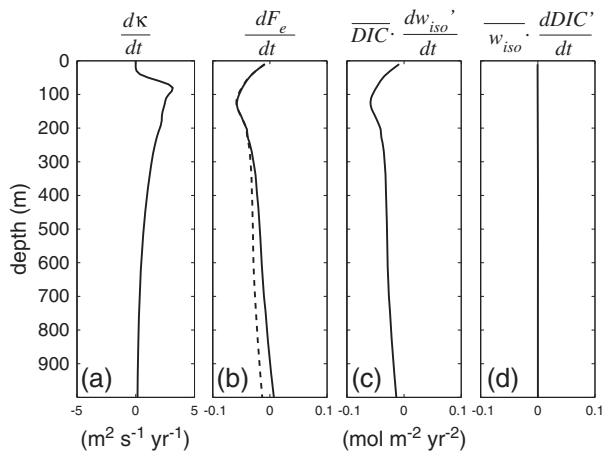


Figure 3. Linear trends in the Southern Ocean averaged (a) eddy-induced advection coefficient, (b) eddy-induced DIC flux, (c) the component of eddy-induced DIC flux associated with variations in vertical isopycnal velocity, and (d) the component of eddy-induced DIC flux associated with variations in DIC. The dashed line in Figure 3b is the sum of Figures 3c and 3d.

tracers along isopycnals by means of a diffusion operator [Redi, 1982]. The second, termed “thickness diffusion”, represents the adiabatic slumping of isopycnal surfaces via mesoscale baroclinic instability. To determine the importance of a variable eddy coefficient, κ , for the Southern Ocean DIC inventory, the effect of this second component is estimated by calculating the eddy-induced flux of DIC, F_e ,

$$F_e = w_{iso}DIC, \quad (2)$$

where w_{iso} is the vertical eddy-induced velocity predicted from the Gent and McWilliams [1990] parameterization. Both κ and F_e exhibit the largest trends in the top 200 m of the water column (Figures 3a and 3b). We quantify the sensitivity of the trend in F_e to the trend in κ by estimating the linear congruence of the trends in these variables in the upper 700 m of the water column (Figure S3). At a depth of 200 m, we find that 92% of the trend in F_e is linearly congruent with the trend in κ .

[10] The cause of the trends in the eddy-induced flux of DIC is determined by separating DIC and w_{iso} into mean and time-varying components:

$$DIC = \overline{DIC} + DIC', w_{iso} = \overline{w_{iso}} + w_{iso}', \quad (3)$$

where the bars represent the long-term mean over the 50 year simulation, and the primes represent monthly deviations from the long-term mean. The linear trend in the eddy-induced DIC flux can therefore be approximated by substituting (3) into (2),

$$\frac{\partial F_e}{\partial t} \approx \overline{DIC} \cdot \frac{\partial w_{iso}'}{\partial t} + \overline{w_{iso}} \cdot \frac{\partial DIC'}{\partial t}, \quad (4)$$

ignoring the prime-prime terms, which are small. Figures 3c and 3d show the components of the eddy-induced DIC flux trend associated with the trends in vertical eddy-induced velocity and DIC, respectively. The sum of these two terms is the dashed profile in Figure 3b, which closely matches the modeled trend in F_e . Changes in F_e are primarily

caused by changes in the eddy-induced velocity, and not changes in the vertical distribution of DIC (Figure 3). F_e is computed as the product of κ and the isopycnal slope, however changes in the latter are small during our simulation. Thus, variations in κ are the primary driver of changes in eddy-induced DIC fluxes.

4. Conclusions

[11] A coarse-resolution ocean model with a variable eddy parameterization coefficient simulates significant multi-decadal trends in the air-sea flux, advection, and mixing of natural carbon in the Southern Ocean from 1958 to 2007, similar to trends reported in other studies [e.g., Lovenduski et al., 2008; Lovenduski and Ito, 2009]. The model predicts an increase in the sea-air flux of natural CO_2 over the 50 year simulation, caused by wind-driven increases in the advection and diapycnal mixing of DIC. The trend toward enhanced outgassing is countered by a significant increase in the eddy-induced advection of DIC, which opposes the Eulerian flow.

[12] Our results suggest that changes in the vertical distribution of DIC play only a minor role in modulating the eddy advection of DIC. Thus, if models can correctly capture changes in the eddy velocity field, their representation of changes in the DIC budget should be accurate. A variable eddy-induced advection coefficient provides a mechanism for eddy fluxes to respond to changing winds. If κ had not increased during the simulation, the result would have been a much smaller eddy-induced flux of DIC throughout the upper water column, resulting in a larger increase in the surface DIC inventory and a greater release of natural CO_2 from 1958 to 2007.

[13] **Acknowledgments.** NSL is grateful for support from NOAA (NA12OAR4310058) and NSF (OCE-1155240). NCAR is sponsored by the National Science Foundation. Computational facilities have been provided by the Climate Simulation Laboratory, which is managed by CISL at NCAR.

References

- Böning, C. W., A. Dispert, M. Visbeck, S. R. Rintoul, and F. U. Schwarzkopf (2008), The response of the Antarctic Circumpolar Current to recent climate change, *Nature Geosci.*, *1*(12), 864–869.
- Danabasoglu, G., et al. (2012), The CCSM4 ocean component, *J. Clim.*, *25*(5), 1361–1389.
- Denman, K. L., et al. (2007), Couplings between changes in the climate system and biogeochemistry, in *Climate Change 2007: The Physical Science Basis. Contribution of Working Group I to the Fourth Assessment Report of the Intergovernmental Panel on Climate Change*, edited by S. Solomon, et al., Cambridge University Press, Cambridge, United Kingdom and New York, NY, USA.
- Doney, S. C., et al. (2009), Mechanisms governing interannual variability in upper-ocean inorganic carbon system and air-sea CO_2 fluxes: Physical climate and atmospheric dust, *Deep Sea Res. II*, *56*(8–10), 640–655.
- Farneti, R., and P. R. Gent (2011), The effects of the eddy-induced advection coefficient in a coarse-resolution coupled climate model, *Ocean Modell.*, *39*(1–2), 135–145.
- Gent, P. R., and G. Danabasoglu (2011), Response to increasing Southern Hemisphere winds in CCSM4, *J. Clim.*, *24*(19), 4992–4998.
- Gent, P. R., and J. C. McWilliams (1990), Isopycnal mixing in ocean circulation models, *J. Phys. Oceanogr.*, *20*(1), 150–155.
- Hogg, A. M. C., M. P. Meredith, J. R. Blundell, and C. Wilson (2008), Eddy heat flux in the Southern Ocean: Response to variable wind forcing, *J. Clim.*, *21*(4), 608–620.
- Le Quéré, C., et al. (2007), Saturation of the Southern Ocean CO_2 sink due to recent climate change, *Science*, *316*(5832), 1735–1738.
- Lovenduski, N. S., and T. Ito (2009), The future evolution of the Southern Ocean CO_2 sink, *J. Mar. Res.*, *67*(5), 597–617, doi:10.1357/002224009791218832.

- Lovenduski, N. S., N. Gruber, and S. C. Doney (2008), Toward a mechanistic understanding of the decadal trends in the Southern Ocean carbon sink, *Global Biogeochem. Cycles*, *22*(3), GB3016, doi:10.1029/2007GB003139.
- Marshall, J., and T. Radko (2003), Residual-mean solutions for the Antarctic Circumpolar Current and its associated overturning circulation, *J. Phys. Oceanogr.*, *33*(11), 2341–2354.
- Moore, J. K., S. C. Doney, and K. Lindsay (2004), Upper ocean ecosystem dynamics and iron cycling in a global three-dimensional model, *Global Biogeochem. Cycles*, *18*(4), GB4028, doi:10.1029/2004GB002220.
- Redi, M. H. (1982), Oceanic isopycnal mixing by coordinate rotation, *J. Phys. Oceanogr.*, *12*(10), 1154–1158.